Developmental Biology 380 (2013) 222–232

Contents lists available at SciVerse ScienceDirect

Developmental Biology

journal homepage: www.elsevier.com/locate/developmentalbiology

# Wnt signaling regulates left–right axis formation in the node of mouse embryos

Keiko Kitajima [a], Shinya Oki [a], Yasuyuki Ohkawa [b], Tomoyuki Sumi [a], Chikara Meno [a,*]

[a] Department of Developmental Biology, Graduate School of Medical Sciences, Kyushu University, 3-1-1 Maidashi, Higashi-ku, Fukuoka 812-8582, Japan
[b] Department of Epigenetics, Graduate School of Medical Sciences, Kyushu University, 3-1-1 Maidashi, Higashi-ku, Fukuoka 812-8582, Japan

ARTICLE INFO

*Article history:*
Received 30 November 2012
Received in revised form
8 May 2013
Accepted 10 May 2013
Available online 21 May 2013

*Keywords:*
Left–right axis
Node
Mouse embryo
Wnt
Notch signaling

ABSTRACT

The node triggers formation of the left–right axis in mouse embryos by establishing local asymmetry of *Nodal* and *Cerl2* expression. We found that *Wnt3* is expressed in perinodal crown cells preferentially on the left side. The enhancer responsible for *Wnt3* expression was identified and found to be regulated by Foxa2 and Rbpj under the control of Notch signaling. Rbpj binding sites suppress enhancer activity in pit cells of the node, thereby ensuring crown cell-specific expression. In addition, we found that the expression of *Gdf1* and *Cerl2* is also regulated by Notch signaling, suggesting that such signaling may induce the expression of genes related to left–right asymmetry as a set. Furthermore, *Cerl2* expression became symmetric in response to inhibition of Wnt-β-catenin signaling. Our results suggest that Wnt signaling regulates the asymmetry of *Cerl2* expression, which likely generates a left–right difference in Nodal activity at the node for further amplification in lateral plate mesoderm.



## Introduction

The left–right (L–R) asymmetry of visceral organs in vertebrates is generated on the basis of the L–R axis established at an early developmental stage (Shiratori and Hamada, 2006). The mouse embryo develops initially as a bilateral structure after acquiring anteroposterior and dorsoventral axes. At the early bud stage, the node is formed at the anterior-most portion of the primitive streak. The ventral layer of the node forms a depression, the periphery and inside of which are composed of crown cells and pit cells, respectively (Bellomo et al., 1996; Sulik et al., 1994). The initial event of L–R axis formation depends on a leftward fluid flow known as nodal flow (McGrath et al., 2003; Nonaka et al., 1998; Tanaka et al., 2005). L–R asymmetry of gene expression appears first in the crown cells of the node as a result of nodal flow. Such asymmetry then becomes apparent in the lateral plate mesoderm (LPM), and robust L–R differences in gene expression are established along the anteroposterior axis (Nakamura et al., 2006; Shiratori and Hamada, 2006).

Nodal, a member of the transforming growth factor-β superfamily of proteins, plays a fundamental role in L–R axis formation. *Nodal* is expressed in the entire left LPM at the early somite stage and thereby imparts left-side identity to LPM (Collignon et al., 1996; Lowe et al., 1996; Meno et al., 1998; Meno et al., 2001; Yan et al., 1999). Establishment of the L–R axis requires elaborate regulation of Nodal signaling. First, the area competent to respond to Nodal signaling is restricted to the LPM, floor plate, and node, where Cryptic, a cofactor of Nodal signaling, is present (Yan et al., 1999). Second, the activity of Nodal is augmented by its formation of a heterodimer with Gdf1, which is expressed in the crown cells of the node and in LPM (Tanaka et al., 2007). Third, Nodal functions in both positive and negative feedback loops. An intronic enhancer (ASE) of *Nodal* is thus activated by Foxh1 under the control of Nodal signaling (Saijoh et al., 2000), and this positive loop expands *Nodal* expression in the left LPM (Norris et al., 2002; Saijoh et al., 2000). In addition, Nodal induces expression of the genes for its own inhibitors, Lefty1 and Lefty2 (Saijoh et al., 2000; Yamamoto et al., 2003), which results in restriction of *Nodal* expression to the left side of the LPM (Meno et al., 1998; Meno et al., 2001; Saijoh et al., 2000; Yamamoto et al., 2003).

*Nodal* is expressed in the crown cells of the node before its expression in the left LPM. *Nodal* expression in the node is regulated by an enhancer designated NDE (node-specific enhancer), which contains binding sites for Rbpj and is activated by Notch signaling (Krebs et al., 2003; Raya et al., 2003). Nodal produced in the node likely diffuses to the LPM and induces its own expression there by the positive feedback loop (Oki et al., 2007). *Nodal* expression in the node is L–R asymmetric, with the level being higher on the left side. Furthermore, the gene for the Nodal antagonist Cerl2 is expressed in crown cells with the opposite L–R asymmetry (Marques et al., 2004, Pearce et al., 1999). Nodal activity is thus probably higher on the left side of

* Corresponding author. Fax: +81 92 642 6260.
*E-mail address:* meno@dev.med.kyushu-u.ac.jp (C. Meno).

0012-1606/$ - see front matter © 2013 Elsevier Inc. All rights reserved.
http://dx.doi.org/10.1016/j.ydbio.2013.05.011

the node, consistent with the observed pattern of Smad2 phosphorylation at the node (Kawasumi et al., 2011). The onset of *Nodal* expression in the LPM results in the expression of Lefty proteins (Nakamura et al., 2006; Norris et al., 2002; Yamamoto et al., 2003), which ensures the unilateral expression of *Nodal* on the left (Nakamura et al., 2006). It is important that the left LPM expresses *Nodal* before the right LPM does. We have proposed that this is likely achieved as a result of the opposite asymmetric expression of *Nodal* and *Cerl*2 in the node and the consequent asymmetry of Nodal activity, which likely ensures that the left LPM receives the signal first (Marques et al., 2004; Oki et al., 2009). The mechanisms responsible for the L–R asymmetric expression of genes in crown cells have remained largely unknown, however.

We now show that *Wnt*3 is expressed in the crown cells of the node, with the level of expression being higher on the left side. We identified the enhancer responsible for *Wnt*3 expression and found that the expression is established by the combined actions of Foxa2 and Rbpj under the control of Notch signaling. Furthermore, Notch signaling was shown to be required for the expression of other L–R axis-related genes in crown cells, suggesting that these genes may share a common mechanism of transcriptional regulation. We found that canonical Wnt signaling suppresses the expression of *Cerl*2, likely explaining the L–R asymmetry of *Cerl*2 expression in the node.

## Materials and methods

### *Generation of BAC transgenic mouse lines*

Mouse BAC (bacterial artificial chromosome) clone RP23-31D10 (BACPAC Resources Center) was modified by recombineering to generate BAC transgenic mouse lines. For the *Wnt*3 enhancer reporter line *Wnt*3$^{\text{NDCE-flox}}$::*lacZ*, IRES (internal ribosome entry site)–*lacZ* was inserted into the 3′ untranslated region of *Wnt*3 (6 bp downstream of the stop codon), and *loxP* and *FRT-loxP* were then inserted 5 bp downstream of exon 2 and 2387 bp upstream of exon 3, respectively. Linearized BAC clones were microinjected into the pronucleus of B6C3F$_1$ fertilized mouse eggs.

The *CAG-CreER*$^{\text{T2}}$ transgenic line was also generated and crossed with *Wnt*3$^{\text{NDCE-flox}}$::*lacZ* transgenic mice to obtain embryos positive for both transgenes. For induction of Cre-mediated recombination, pregnant females were administered tamoxifen (0.1 mg per gram of body weight) dissolved in corn oil by oral gavage at embryonic day (*E*) 6.5, and embryos were collected at E8.2. The study was approved by the Animal Care and Use Committee of Kyushu University.

### *lacZ constructs for exploration of the Wnt3 enhancer*

Approximately 10-kbp fragments (designated #1 to #5) encompassing the *Wnt*3 locus were generated from RP23-31D10. Fragment #4 was further subdivided by conventional methods based on restriction enzymes or the polymerase chain reaction (PCR). Mutations were introduced into the Rbpj or Foxa2 binding sites of the *Wnt*3 enhancer (NDCE) or the *Nodal* enhancer (NDE) with the use of PCR-based mutagenesis. *Wnt*3 NDCE or *Nodal* NDE (chromosome 10 positions 60870456–60871353, amplified by PCR) in pBS-KS was used as the template (Supplementary Table S1). The various DNA fragments were joined to *lacZ* and placed under the control of the mouse *Wnt*3 or *Hsp*68 promoters.

### *Genotyping of transgenic mice*

To identify transgenic embryos or mice, we isolated genomic DNA from embryos by proteinase K treatment or from the tail of mice with the use of a REDExtract-N-Amp Tissue PCR kit (Sigma-Aldrich). The DNA preparations were then subjected to PCR analysis with specific primers (Supplementary Table S1).

### *Whole-mount in situ hybridization*

Whole-mount in situ hybridization was performed according to standard procedures. Female ICR mice were mated with male ICR mice or *Wnt*3$^{\text{NDCE-flox}}$::*lacZ* transgenic mice (B6/C3H hybrid) to obtain embryos. For two-color analysis, embryos were subjected to simultaneous hybridization with digoxigenin- and fluorescein-labeled probes. Both probes were successively detected with alkaline phosphatase-conjugated antibodies. The first color was developed with NBT/BCIP (Roche). After inactivation of alkaline phosphatase at 70 °C, the second antibody was applied and the color was developed with INT/BCIP (Roche). Experiments were always performed with control embryos, and the color was developed with the same stop time for comparison.

### *EMSA analysis*

For construction of tagged Foxa2 and Rbpj (Chen et al., 2011; Lubman et al., 2007), the open reading frames of mouse Foxa2 and Rbpj cDNAs were inserted into pCMV-Tag3 and p3 × FLAG-CMV, respectively. Nuclear extracts containing Foxa2 or Rbpj were prepared from human embryonic kidney 293T (HEK293T) cells that had been transfected with the expression vectors encoding Myc-Foxa2 or 3 × FLAG-Rbpj by the calcium phosphate method. Electrophoretic mobility-shift assay (EMSA) analysis was performed as previously described (Scott et al., 1994). For supershift analysis, normal mouse immunoglobulin G (IgG) (Sigma), antibodies to Myc (9E10, Biomol), or antibodies to FLAG (M2, Sigma) were added to the reaction mixture containing the nuclear extract and probe before electrophoresis.

### *Luciferase reporter assay*

HeLa cells were transfected with pGL3 (Promega) containing *Wnt*3 NDCE as well as with expression vectors for Myc-Foxa2, 3 × FLAG-Rbpj, or the intracellular domain of mouse Notch1 (NICD) (Kato et al., 1996; Mizushima and Nagata, 1990). The cells were also transfected with pEF-β geo for normalization of transfection efficiency. Cell extracts were prepared and assayed for luciferase and β-galactosidase activities 24 h after transfection with the use of a luciferase assay system (Promega).

### *Whole-embryo culture*

Mouse embryos at E7.7 were cultured under a humidified atmosphere of 5% $CO_2$ at 37 °C in Dulbecco's modified Eagle's medium (DMEM) supplemented with 75% rat serum. For forced expression of Foxa2, an expression plasmid encoding Myc-Foxa2 was combined with Lipofectamine 2000 (Invitrogen) and injected through a glass needle with an injector (Narishige) into the presomitic mesoderm immediately beneath the visceral endoderm layer of embryos at the late headfold (LHF) stage. For modulation of canonical Wnt signaling or Notch signaling pathways, embryos were cultured from the LHF or one-somite stage to the three-somite stage in medium containing 225 μM XAV939 (Sigma), 20 μM CHIR99021 (Cayman Chemicals), 40 μM *N*-[*N*-(3,5-difluorophenacetyl)-L-alanyl]-*S*-phenylglycine *t*-butyl ester (DAPT) (Sigma), or dimethyl sulfoxide (control). For the observation of nodal flow, the node region of cultured embryos was excised and placed in a chamber that consisted of a microscope slide and a silicone sheet with a hole and which was filled with HEPES-buffered DMEM supplemented with 10% fetal bovine serum and

1.00-μm-diameter microspheres (Polysciences). After placement of a cover slip, the movement of the microspheres was recorded with the use of an inverted microscope equipped with a digital camera (DS-2Mv, Nikon).

## Results

### *L–R asymmetric expression of Wnt3 in perinodal crown cells*

During investigation of a possible role for Wnt signaling in the regulation of L–R axis formation, we found that *Wnt3* is L–R asymmetrically expressed in the crown cells of the node. The L–R asymmetric expression of *Wnt3* became apparent during the transition from the LHF stage to the one-somite stage, with the expression level being higher on the left side ($n=13$ out of 29 embryos) (Fig. 1A and B). The asymmetric pattern was also observed in almost half of all embryos at the two-somite stage ($n=5/13$) (Fig. 1C), and it was detected in all embryos thereafter ($n=19$ at the three-somite stage) (Fig. 1D). For comparison, we examined the expression of *Nodal* as well as the gene for the Nodal inhibitor Cerl2 in the node from the LHF to three-somite stages. Expression of *Nodal* and *Cerl2* becomes asymmetric from the two-somite stage, with that of *Nodal* being stronger on the left side (Fig. 1E–H) (Collignon et al., 1996; Lowe et al., 1996) and that of *Cerl2* stronger on the right (Fig. 1I–L and Supplementary Fig. S1) (Marques et al., 2004; Oki et al., 2009). These results suggested that the asymmetric expression of *Wnt3* precedes that of *Nodal* and *Cerl2*.

### *A node-specific enhancer in intron 2 of Wnt3*

We next explored the transcriptional regulatory elements responsible for *Wnt3* expression in the node. We divided ~60 kbp of the *Wnt3* locus into five regions (#1 to #5) (Fig. 2A), linked each region to the *Wnt3* promoter and *lacZ*, and injected the resulting reporter constructs into the pronucleus of fertilized mouse eggs. The resulting embryos were allowed to develop in utero until E8.5 and were then subjected to X-gal (5-bromo-4-chloro-3-indoyl-β-D-galactoside) staining in order to detect expression of each *lacZ* transgene. An 11-kbp region upstream of the transcription start site of *Wnt3* (fragment #1) showed enhancer activity only in the dorsal neural tube, whereas the activity of a 9.2-kbp region immediately downstream of *Wnt3* exon 1 (fragment #2) was detected only in the limb bud and tail bud at E9.5 (Fig. 2A; data not shown). The next 11.0-kbp region (fragment #3) and a downstream 8.5-kbp region containing *Wnt3* exons 3, 4, and 5 (fragment #5) did not confer *lacZ* expression at E8.5 (Fig. 2A). We found that the node enhancer is located in a 9.3-kbp region (fragment #4) containing exon 2. X-gal staining was observed in crown cells in two of five transgene-positive embryos, with one embryo exhibiting L–R asymmetry with a L > R staining pattern (Fig. 2A).

To further delineate the position of the enhancer, we performed deletion analysis of fragment #4 (Fig. 2B). Deletion of the 5′ region alone (fragments AH7.0 and HH4.0) or together with an additional 1.2-kbp 3′ region (fragment HK2.8) did not affect enhancer activity. Given that fragment PK1.7 still manifested enhancer activity in the node but with a reduced strength (Fig. 2B), we substituted the *Hsp*68 promoter for the native *Wnt3* promoter in subsequent assays. We thereby further narrowed the enhancer region to a 0.9-kbp fragment that includes a portion of exon 2, with the corresponding construct (PX0.9-*lacZ*) showing enhancer activity in the node. Examination of the L–R asymmetric activity of PX0.9 at the one- to five-somite stages revealed that X-gal staining tended to be stronger on the left side (L > R, $n=2/5$; L=R, $n=2/5$; not determined because of additional ectopic staining, $n=1/5$). Furthermore, internal deletion of this 0.9-kbp region from fragment #4 (to give fragment ΔPX0.9) abolished *lacZ* expression in the node (Fig. 2B). These results thus showed that the cis-regulatory elements for *Wnt3* expression in the node are located adjacent to exon 2, at a position ~43 kbp downstream of the transcription start site. We named this enhancer the node crown cell enhancer (NDCE).

To confirm that *Wnt3* expression in the node depends on NDCE, we generated transgenic mice harboring a *lacZ* reporter construct lacking the enhancer. We thus inserted an IRES-*lacZ* element into

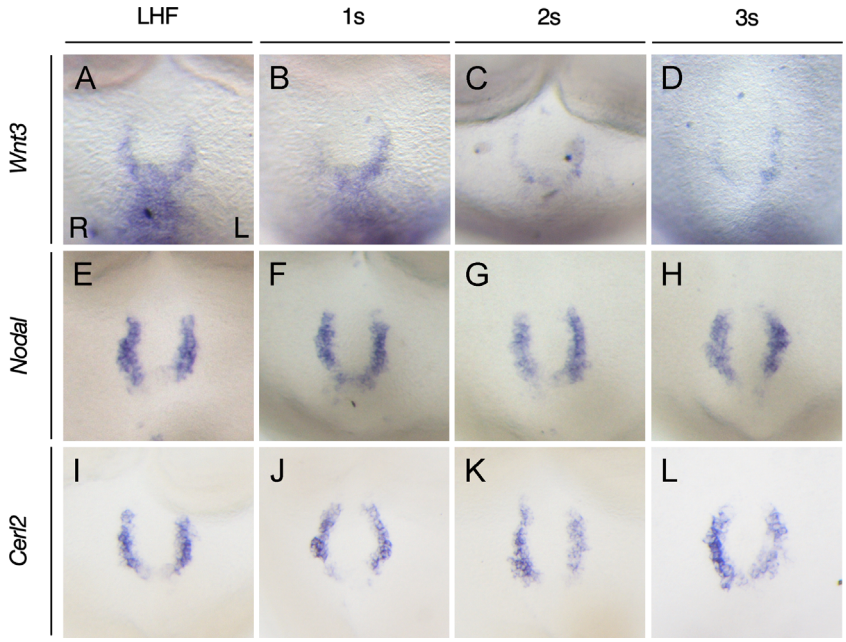


**Fig. 1.** Expression of *Wnt3*, *Nodal*, and *Cerl2* in the node. Expression of *Wnt3* (A–D), *Nodal* (E–H), and *Cerl2* (I–L) at the LHF (A, E, I), one-somite (1s) (B, F, J), two-somite (C, G, K), and three-somite (D, H, L) stages of the ICR mouse embryo was examined by whole-mount in situ hybridization. The node region is shown with anterior at the top.

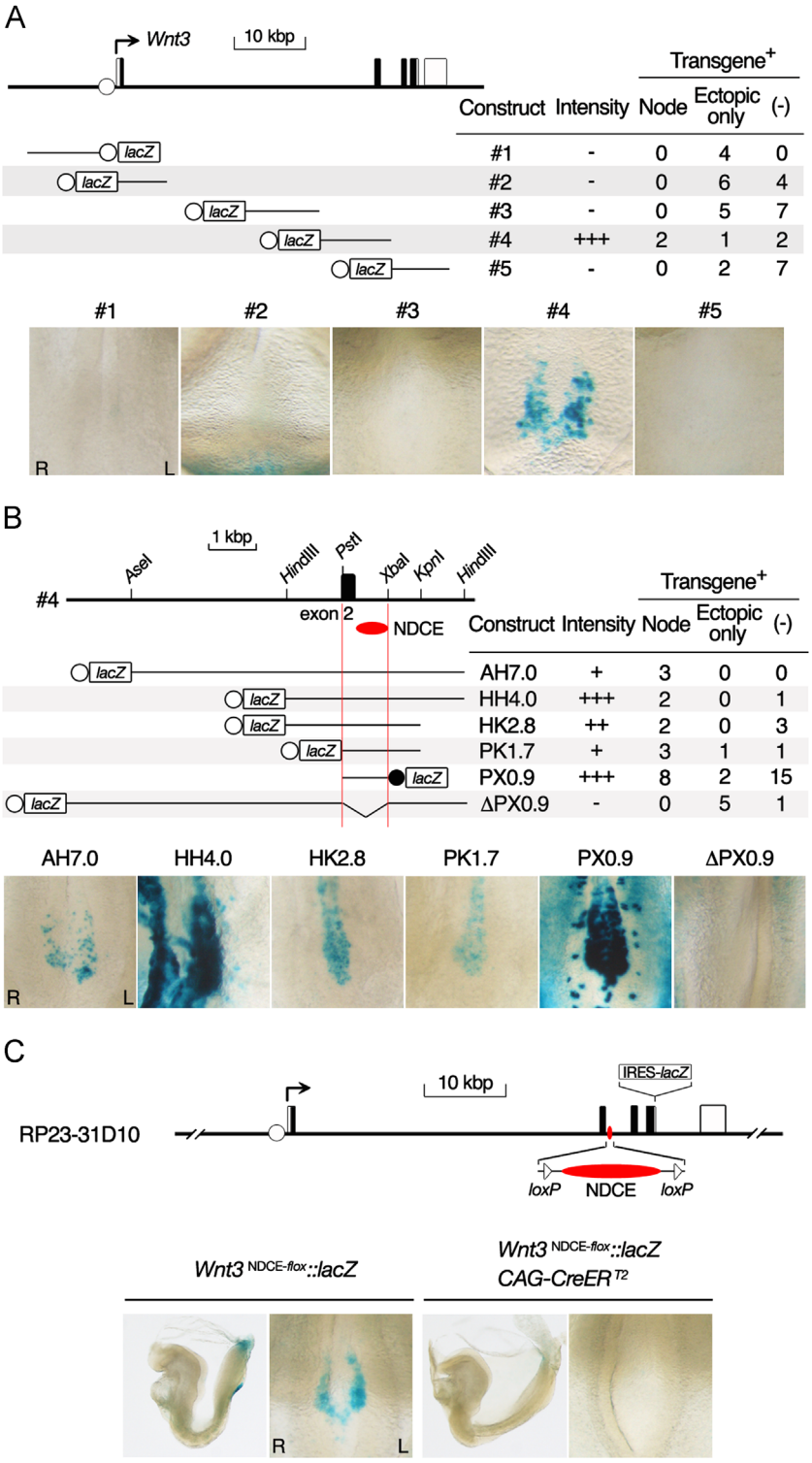


**Fig. 2.** Identification of the enhancer responsible for *Wnt3* expression in the node. (A) The *Wnt3* locus and *lacZ* reporter constructs for transgenic assays are shown at the top left. Open circles represent the *Wnt3* promoter. The table shows the pattern of X-gal staining and the intensity of staining in the node for each construct. Transgene-positive embryos were classified according to the staining pattern observed at E8.5: node, node-specific staining; ectopic only, staining not correlated with endogenous *Wnt3* expression; (–), no staining. The numbers of embryos with each pattern are indicated. Representative X-gal staining patterns around the node of transgenic embryos harboring the indicated constructs are also shown; anterior is to the top. (B) Fragment #4 of the *Wnt3* locus was subdivided by restriction enzymes, and the enhancer activity of each region was determined as in (A). Open and closed circles represent *Wnt3* and *Hsp*68 promoters, respectively. (C) The BAC transgenic mouse line *Wnt3*$^{NDCE\text{-}flox}$::*lacZ* was generated to examine the enhancer activity of NDCE. *Wnt3*$^{NDCE\text{-}flox}$::*lacZ* mice were crossed with *CAG-CreER*$^{T2}$ mice, and the resulting embryos were exposed to tamoxifen in utero at E6.5 and were examined for X-gal staining in the node at E8.2. Lateral views of littermate embryos and enlarged views of the node are shown on the left and right, respectively, of each pair of images.

a BAC clone (RP23-31D10) immediately downstream of the *Wnt3* stop codon in exon 4 in order to monitor *Wnt3* expression, and we sandwiched NDCE between *loxP* sites (to yield RP23-31D10 *Wnt3*$^{NDCE\text{-}flox}$::*lacZ*). Transgenic embryos at the early somite stage manifested asymmetric X-gal staining in the node, recapitulating the endogenous expression pattern of *Wnt3* (Fig. 2C). We then

crossed these transgenic mice with *CAG-CreER*$^{T2}$ mice, which ubiquitously express a gene for inducible Cre recombinase. Exposure of the resulting embryos to tamoxifen resulted in the complete loss of X-gal staining in the node (Fig. 2C), indicating that *Wnt3* expression in the node is driven by NDCE.

### *Deletion mapping of Wnt3 regulatory elements*

To identify core elements underlying enhancer activity, we linked various deletion fragments of NDCE to the *Hsp68-lacZ* construct and examined their activity in transgenic assays (Fig. 3A). A database (MatBase) search suggested that NDCE includes potential binding sites for Foxa2 and Rbpj, the latter a primary transcriptional mediator of Notch signaling, with the binding site for Foxa2 being located between 5′ and 3′ Rbpj sites (Overdier et al., 1994; Tun et al., 1994). In the case of the 3′ deletion constructs, enhancer activity was preserved if they included the Foxa2 binding site (constructs 5′-650 and 5′-625) but not if they did not (construct 5′-610) (Fig. 3A). Of the 5′-315 and 3′-366 fragments, which contain the 5′ Rbpj binding site and both the Foxa2 and 3′ Rbpj sites, respectively, only the latter exhibited enhancer activity (Fig. 3A). These results thus suggested that the Foxa2 binding site is necessary for *Wnt3* expression in the node.

### *Combined activities of Foxa2 and Rbpj induce Wnt3 and Nodal expression in perinodal crown cells*

To confirm that the Foxa2 binding site is a core element of NDCE, we generated transgenic embryos harboring PX0.9-*lacZ* with a mutated Foxa2 site (NDCEΔF) (Fig. 3B). Out of nine transgenic embryos obtained, two embryos showed weak X-gal staining in node crown cells (Fig. 3C), suggesting that the Foxa2 binding site is required

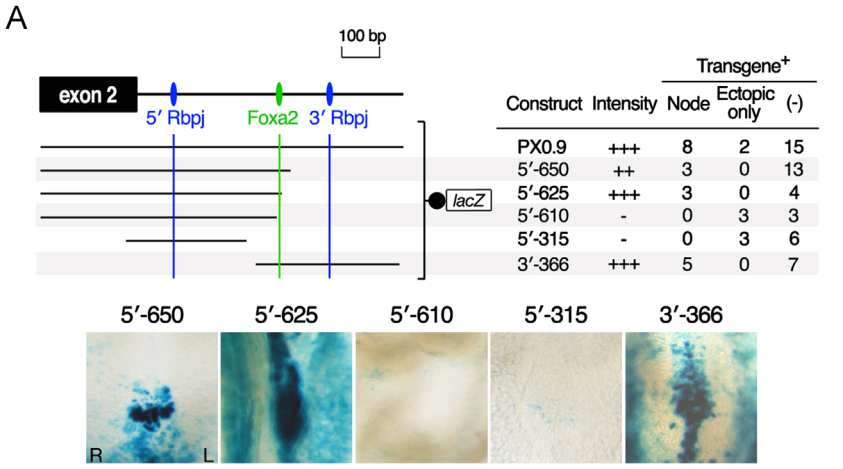


| Construct | Intensity | Transgene+ Node | Ectopic only | (-) |
|---|---|---|---|---|
| PX0.9 | +++ | 8 | 2 | 15 |
| 5′-650 | ++ | 3 | 0 | 13 |
| 5′-625 | +++ | 3 | 0 | 4 |
| 5′-610 | - | 0 | 3 | 3 |
| 5′-315 | - | 0 | 3 | 6 |
| 3′-366 | +++ | 5 | 0 | 7 |

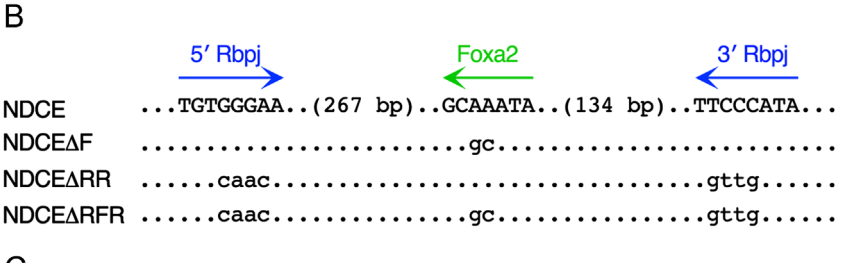


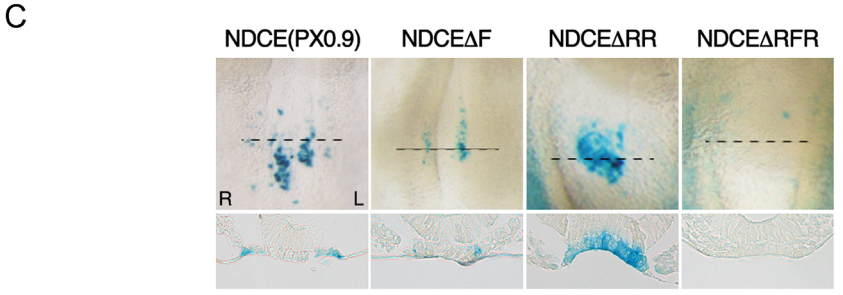


| | | | | |
|---|---|---|---|---|
| Crown cells only | 4 | 2 | 0 | 0 |
| Crown cells + pit cells | 1 | 0 | 8 | 0 |
| Ectopic only | 0 | 0 | 0 | 7 |
| None | 12 | 7 | 6 | 2 |

**Fig. 3.** Foxa2 and Rbpj binding sites are required for *Wnt3* expression in crown cells. (A) Various deletion constructs of NDCE were examined in transgenic assays in order to identify the core elements for *Wnt3* enhancer activity. Construct names indicate the size of genomic fragments in base pairs. Representative X-gal staining patterns around the node at E8.5 and a summary of the staining patterns observed for each construct are shown. (B) Consensus sequences for binding of Foxa2 and Rbpj in NDCE. Three types of *lacZ* construct with point mutations in the putative binding site for Foxa2 (ΔF), in both those for Rbpj (ΔRR), or in all three sites (ΔRFR) were generated. (C) Effect of point mutations on enhancer activity. Representative X-gal staining patterns around the node of E8.5 transgenic embryos harboring the mutated enhancer constructs are shown in ventral views and sections at the indicated lines together with a summary of the staining patterns observed for each construct. Only embryos at the one- to five-somite stages were counted for this summary in order to allow staining in crown cells to be distinguished from that in pit cells.

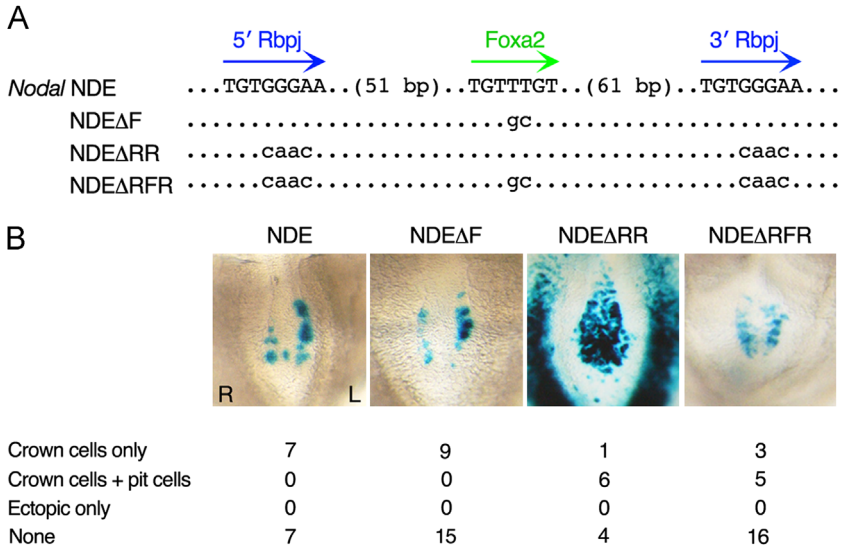


| | NDE | NDEΔF | NDEΔRR | NDEΔRFR |
|---|---|---|---|---|
| Crown cells only | 7 | 9 | 1 | 3 |
| Crown cells + pit cells | 0 | 0 | 6 | 5 |
| Ectopic only | 0 | 0 | 0 | 0 |
| None | 7 | 15 | 4 | 16 |

**Fig. 4.** Rbpj binding sites in the NDE of *Nodal* are required to suppress enhancer activity in pit cells. (A) Consensus sequences for the binding of Foxa2 and Rbpj in *Nodal* NDE. Three types of *lacZ* construct with point mutations in the putative binding site for Foxa2 (ΔF), in both those for Rbpj (ΔRR), or in all three sites (ΔRFR) were generated. (B) Effect of point mutations on enhancer activity. Representative X-gal staining patterns around the node of E8.5 transgenic embryos harboring the mutated enhancer constructs are shown in ventral views together with a summary of the staining patterns observed for each construct. Only embryos at the one- to five-somite stages were counted for this summary in order to allow staining in crown cells to be distinguished from that in pit cells.

for full activity of NDCE. Given that *Nodal* expression in the node is induced by Notch signaling via Rbpj binding sites, we also introduced mutations into the two Rbpj binding sites of NDCE (Fig. 3B). X-gal staining in the node was not observed in transgenic embryos harboring PX0.9-*lacZ* with mutations in the two Rbpj binding sites as well as in the Foxa2 site (NDCEΔRFR construct) ($n=9$) (Fig. 3C), indicating that both types of site are required for enhancer activity. Furthermore, we found that mutation of only the two Rbpj binding sites (NDCEΔRR construct) resulted in the appearance of X-gal staining in pit cells as well as in crown cells (Fig. 3B and C), with *Foxa2* being expressed in both types of node cells (Supplementary Fig. S2) (Sasaki and Hogan, 1993). Rbpj recruits corepressors to silence gene expression in the absence of Notch signaling (Borggrefe and Oswald, 2009). This appearance of enhancer activity in pit cells thus suggests that Rbpj normally antagonizes Foxa2 activity in the pit cells. On the other hand, in the crown cells, where Notch signaling occurs, Rbpj and Foxa2 likely increase NDCE activity and thereby establish the horseshoe-shaped expression pattern of *Wnt3*.

*Nodal* expression in the node is regulated by the enhancer NDE, whose activity is controlled by two consensus binding sites for Rbpj (Krebs et al., 2003; Raya et al., 2003). Given that a Foxa2 binding site in NDE is conserved among species (Brennan et al., 2002), we examined the possible role of this Foxa2 binding site in *Nodal* expression in the node. We compared X-gal staining patterns among transgenic embryos harboring NDE-*Hsp*68-*lacZ* constructs with mutations in the Foxa2 binding site (NDEΔF), in both Rbpj binding sites (NDEΔRR), or in all three sites (NDEΔRFR) (Fig. 4A). The enhancer activity of NDEΔF was not diminished compared with that of NDE (Fig. 4B). As expected, mutation of the two Rbpj binding sites of NDE (NDEΔRR construct) resulted in a high level of X-gal staining not only in crown cells but also in pit cells (Fig. 4B). Unexpectedly, however, in NDEΔRFR-*Hsp*68-*lacZ* embryos, X-gal staining was still observed in a horseshoe pattern, although the boundary of the staining between crown cells and pit cells was less distinct than that in NDE-*Hsp*68-*lacZ* or NDEΔF-*Hsp*68-*lacZ* embryos (Fig. 4B). These results suggested that the two Rbpj binding sites of *Nodal* NDE suppress enhancer activity mediated by the Foxa2 binding site in pit cells, and that unknown elements also contribute to the activity of *Nodal* NDE in addition to the Foxa2 and Rbpj binding sites.

### *EMSA analysis of Foxa2 and Rbpj binding sites in the Wnt3 enhancer*

To examine whether Foxa2 and Rbpj are capable of binding to the potential binding sites in *Wnt3* NDCE, we performed electrophoretic mobility-shift assays (EMSAs) with nuclear extracts prepared from human embryonic kidney 293T (HEK293T) cells expressing Myc epitope-tagged Foxa2 or 3 × FLAG-tagged Rbpj. Double-stranded oligonucleotide probes including the 5′ or 3′ Rbpj binding sites of NDCE (Fig. 5A) manifested a shift in mobility in the presence of the nuclear extract containing 3 × FLAG-Rbpj (Fig. 5B). Similarly, an oligonucleotide probe including the Foxa2 binding site of NDCE was shifted in the presence of the nuclear extract containing Myc-Foxa2 (Fig. 5B). In addition, antibodies to either the Myc or FLAG tags further retarded the electrophoretic mobility of the corresponding probe-protein complexes (Fig. 5B), indicating that Myc-Foxa2 and 3 × FLAG-Rbpj are able to bind to *Wnt3* NDCE in vitro.

### *Combinatorial effects of Foxa2 and Rbpj in activation of Wnt3 NDCE*

To evaluate the transactivation activity of Foxa2 and Rbpj at *Wnt3* NDCE in vivo, we performed a luciferase reporter assay in HeLa cells (Fig. 5C). The cells were thus transfected with the pGL3 reporter plasmid containing NDCE together with expression vectors for Myc-Foxa2 or 3 × FLAG-Rbpj. Forced expression of Foxa2 induced a 2.1-fold increase in luciferase activity. In contrast, forced expression of Rbpj, of the intracellular domain of mouse Notch1 (NICD), or of Rbpj plus NICD did not affect transcriptional activity, suggesting that the enhancer activity of *Wnt3* NDCE requires Foxa2. Luciferase activity was increased 3.2-fold in cells expressing both Rbpj and Foxa2, and it was increased 8.7-fold in the additional presence of NICD. These results thus indicated that Foxa2 and Notch-Rbpj signaling synergistically activate NDCE of *Wnt3*.

### *Notch signaling regulates the expression of Wnt3 and node-specific genes*

To address whether Notch signaling is required for *Wnt3* expression in mouse embryos, we performed whole-embryo culture in the presence of DAPT, a specific inhibitor of γ-secretase,

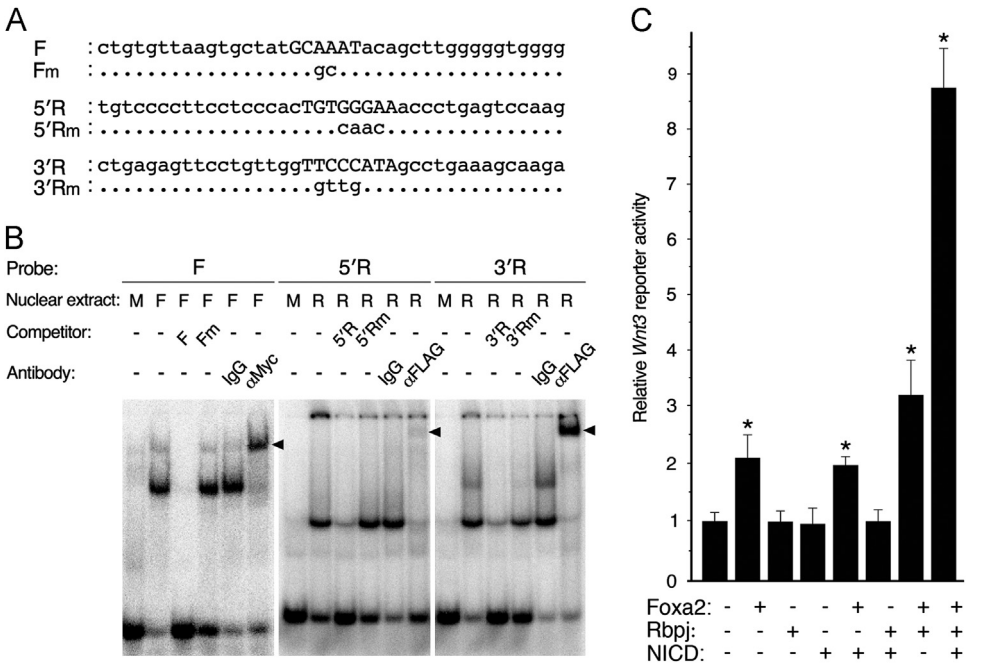


**Fig. 5.** *Wnt3* NDCE is activated by Foxa2 and Notch-Rbpj signaling. (A) Oligonucleotide probes including the Foxa2 (F) or Rbpj (5′R or 3′R) binding sites of *Wnt3* NDCE and their corresponding mutant versions (Fm, 5′Rm, and 3′Rm). (B) EMSA analysis with the oligonucleotide probes in (A) and with nuclear extracts of mock-transfected (M) HEK293T cells or of those transfected with expression vectors for Myc epitope-tagged Foxa2 (F) or 3 × FLAG-tagged Rbpj (R). A 100-fold excess of unlabeled double-stranded wild-type or mutated oligonucleotide was added to the reaction mixture as a competitor. Competitor oligonucleotides inhibited the observed mobility shifts in a manner dependent on the corresponding intact Foxa2 or Rbpj binding sites. Supershift analysis was performed by including either normal mouse IgG, antibodies to Myc (αMyc), or antibodies to FLAG (αFLAG) in the EMSA reactions. The supershifted bands are indicated by arrowheads. Although the intensity of the supershifted band is low for 5′R, the marked decrease in the intensity of the original band suggests that the antibody specifically inhibited complex formation. (C) HeLa cells were transfected with a luciferase reporter plasmid containing *Wnt3* NDCE together with expression vectors encoding Foxa2, Rbpj, or NICD, as indicated. Luciferase activity in cell lysates was measured after transfection for 24 h. Data are normalized, expressed relative to the control value for cells transfected with the reporter plasmid alone, and are means ± s.d. from three independent experiments. $^{*}P < 0.001$ versus the control value (one-way ANOVA followed by Dunnett's post hoc test).

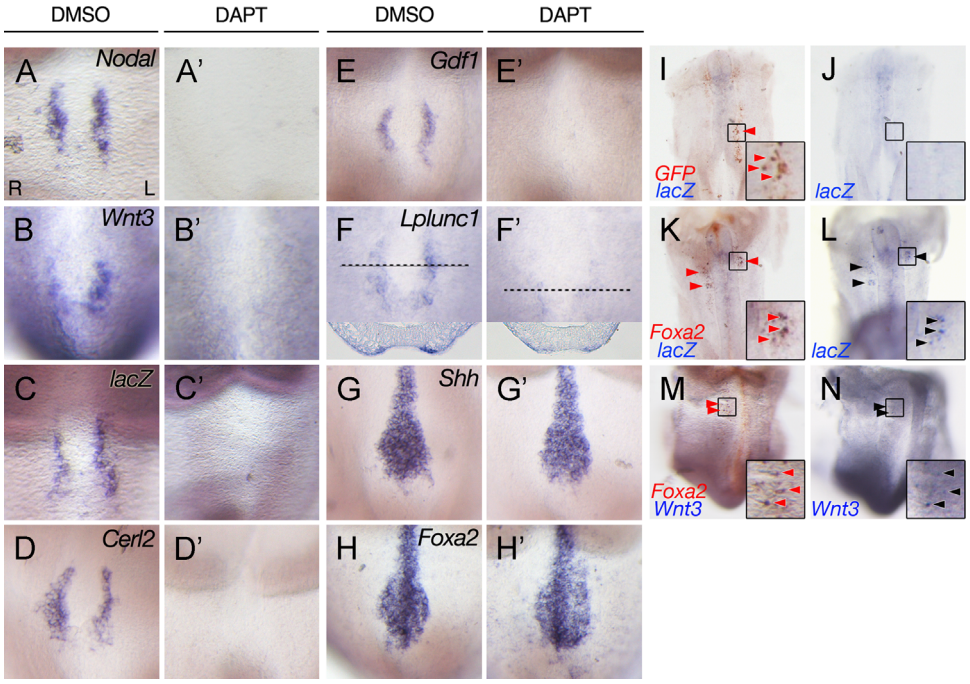


**Fig. 6.** Expression of genes related to L–R asymmetry in crown cells depends on Notch signaling. (A–H, A′–H′) Whole-mount in situ hybridization analysis of the expression of *Nodal* (A, A′), of *Wnt3* (B, B′), of *lacZ* as a reporter for *Wnt3* (C, C′), of *Cerl2* (D, D′), of *Gdf1* (E, E′), of *Lplunc1* (F, F′), of *Shh* (G, G′), and of *Foxa2* (H, H′) in wild-type (B, B′, F, F′) or *Wnt3*$^{\text{NDCE-flox}}$::*lacZ* transgenic (A, A′, C–E, C′–E′, G, G′, H, H′) embryos after culture from the LHF stage to the three-somite stage in the presence of dimethyl sulfoxide (DMSO) vehicle (A–H) or DAPT (A′–H′). The node region is shown with anterior to the top. Lower panels in (F) and (F′) are sections through the node at the indicted line. (I–N) Whole-mount in situ hybridization analysis of the expression of *EGFP* (red) (I), of *Foxa2* (red) (K, M), of *Wnt3* (blue) (M, N), and of *lacZ* as a reporter for *Wnt3* (blue) (I–L) in wild-type (M, N) or *Wnt3*$^{\text{NDCE-flox}}$::*lacZ* transgenic (I–L) embryos after local transfection of presomitic mesoderm at the LHF stage with expression vectors for EGFP (I, J) or Foxa2 (K–N) followed by culture for 16 h. Ventral views are shown with anterior to the top. Enlarged views of the boxed regions are shown in the insets at the bottom right of each panel. (J, L, N) Embryos in (I), (K), and (M) were treated with methanol to eliminate the red color. Arrowheads indicate ectopic induction of *EGFP* or *Foxa2* (red) or of *Wnt3* or *lacZ* (black).

in order to block Notch signaling (Morohashi et al., 2006). We first determined the appropriate concentration of DAPT in culture medium, finding that 40 μM DAPT eliminated *Nodal* expression in the node without affecting embryo morphology ($n=8$) (Fig. 6A and A′). We then cultured wild-type or *Wnt3*$^{NDCE\text{-}flox}$::*lacZ* transgenic embryos at the LHF stage to the three-somite stage in the absence or presence of 40 μM DAPT, after which the embryos were evaluated for expression of *Wnt3* or the *lacZ* transgene as a reporter for *Wnt3* as well as for that of other node marker genes. Whereas control embryos expressed *Wnt3*, *lacZ*, *Nodal*, *Cerl2*, and *Gdf1* in crown cells as well as *Foxa2* and *Shh* in the node, the embryos treated with DAPT completely lost the expression of *Wnt3* and *lacZ* ($n=5$ and 6, respectively) (Fig. 6B, B′, C, and C′) as well as that of *Nodal*. Unexpectedly, the expression of *Cerl2* and *Gdf1* was also lost in DAPT-treated embryos ($n=7$ and 5, respectively) (Fig. 6D, D′, E, and E′). The expression of *Lplunc1*, a gene expressed asymmetrically in crown cells, was also down-regulated by DAPT treatment with the asymmetry being maintained (Fig. 6F and F′). On the other hand, DAPT had no apparent effects on the expression of *Shh* and *Foxa2* in the node, suggesting that the node was formed normally in the presence of DAPT (Fig. 6G, G′, H, and H′). These results together suggested that Notch signaling may induce the expression of *Cerl2*, *Gdf1*, and *Lplunc1* in addition to that of *Wnt3* and *Nodal*, with all of these genes being expressed in a horseshoe-shaped pattern in the node.

### *Forced expression of Foxa2 induces ectopic Wnt3 expression*

To examine whether Foxa2 is able to induce *Wnt3* expression in mouse embryos, we locally introduced a Foxa2 expression vector by lipofection into presomitic mesoderm of embryos at the LHF stage, a tissue in which Notch signaling has been shown to be active (Feller et al., 2008). Transfected wild-type or *Wnt3*$^{NDCE\text{-}flox}$::*lacZ* transgenic embryos were cultured for 16 h and then analyzed by two-color in situ hybridization for expression of *Wnt3*, *lacZ*, and *Foxa2*. Cells ectopically expressing *Foxa2* were found in the paraxial mesoderm along the midline, and the expression of *Wnt3* or *lacZ* was also detected among these cells ($n=7/15$ wild-type embryos and 20/23 transgenic embryos, respectively) (Fig. 6K–N). On the other hand, ectopic *Wnt3* or *lacZ* expression was not observed in control embryos transfected with an expression vector for enhanced green fluorescent protein (EGFP) ($n=15$ and 21, respectively) (Fig. 6I and J), suggesting that Foxa2 is able to induce the expression of *Wnt3* in mouse embryos.

### *Canonical Wnt signaling regulates Cerl2 expression in crown cells*

Given that Wnt3 is considered a canonical Wnt ligand, we next examined whether the canonical Wnt signaling pathway regulates asymmetric gene expression in the node with the use of XAV939, a Tankyrase inhibitor that attenuates Wnt-β-catenin signaling (Huang et al., 2009). Embryos at the one-somite stage were cultured with or without 225 μM XAV939 until the three-somite stage and were then subjected to in situ hybridization analysis. An asymmetry of β-catenin localization has previously been found to develop transiently in the node, with its abundance being higher on the left (Nakaya et al., 2005), suggestive of an asymmetry in Wnt signaling. Despite the short culture period, XAV939 would be expected to reduce the level of such asymmetric signaling. *Foxa2* and *Notch2* were normally expressed in the embryos treated with XAV939 (Fig. 7A, A′, B, and B′). In addition, the expression of *Foxj1*, which is induced by Wnt-β-catenin signaling during ciliogenesis in zebrafish and *Xenopus* (Caron et al., 2012; Walentek et al., 2012), appeared normal in the presence of XAV939 (Fig. 7C and C′). Indeed, nodal flow in XAV939-treated embryos was found to be similar to that in control embryos (Supplementary Videos ce:cross-refs id="crs0095" refid="ec0005 ec0010">1 and 2), suggesting that formation of the node and cilia were not affected by XAV939 in our system. The expression level of *Dll1*, which encodes a Notch ligand and is down-regulated in *Wnt3a* mutant embryos (Nakaya et al., 2005), was slightly reduced in XAV939-treated embryos (Fig. 7D and D′). Nevertheless, neither the level of expression of *Nodal* and *Gdf1*, which is induced by Notch signaling, nor its L–R asymmetry appeared to be affected by XAV939 (Fig. 7E, E′, F, and F′). Importantly, we found that *Cerl2* expression became symmetric and augmented in about half of XAV939-treated embryos ($L=R$, $n=6/10$; $L<R$, $n=4/10$), compared with that in control embryos ($L<R$, $n=5/5$) (Fig. 7G and G′). Consistent with this observation, CHIR99021, an inhibitor of glycogen synthase kinase 3 that activates canonical Wnt signaling (Bain et al., 2007), attenuated the expression of *Cerl2* in the node while maintaining its asymmetry ($n=5/5$) (Fig. 7J and J′). These results thus suggested that canonical Wnt signaling may contribute to the suppression of *Cerl2* expression and to the consequent generation of the right side–dominant expression pattern. Furthermore, expression of *Wnt3* in wild-type embryos and of *lacZ* in *Wnt3*$^{NDCE\text{-}flox}$::*lacZ* embryos was nearly abolished by XAV939 treatment ($n=5/6$ and 10/10, respectively) (Fig. 7H, H′, I, and I′), suggesting that *Wnt3* expression may be markedly influenced by the slight reduction in the level of Notch signaling or that Wnt3 contributes to a positive feedback loop in the regulation of canonical Wnt signaling.

Supplementary material related to this article can be found online at http://dx.doi.org/10.1016/j.ydbio.2013.05.011.

## Discussion

We identified Wnt3 as a secreted factor expressed in crown cells of the node. Secreted factors expressed in this manner are potential regulators of L–R axis formation and also include Nodal, Cerl2, and Gdf1. Targeted mutagenesis of the corresponding genes thus induces L–R laterality defects in mice (Brennan et al., 2002; Marques et al., 2004; Rankin et al., 2000; Tanaka et al., 2007). Although analysis of *Wnt3* by conditional knockout remains to be performed, we have shown here that the canonical Wnt pathway regulates the asymmetry of *Cerl2* expression in the node. Nodal produced in the crown cells likely diffuses via the extracellular matrix to induce *Nodal* expression in LPM (Brennan et al., 2002; Oki et al., 2007; Saijoh et al., 2003). On receipt of the Nodal signal, the left LPM not only expands its *Nodal* expression domain but also represses *Nodal* expression in the right LPM. It is thus important for establishment of the L–R axis that the LPM on the left side responds to the Nodal signal earlier than does that on the right side (Nakamura et al., 2006). The node seems ideally adapted as an asymmetric source of Nodal in this system. First, the crown cells are arranged in a horseshoe pattern, so that the distribution of Nodal may be simply determined by the difference in the amount of active Nodal between the left and right sides. Second, the crown cells interact with adjacent tissue to generate crown cell-specific gene expression. Third, transcription in the crown cells is differentially regulated on the left and right sides under the influence of nodal flow. The mechanisms regulating the amount and activity of Nodal are thus likely to be operative in the crown cells of the node, with many genes expressed in the crown cells contributing to this regulation.

Expression of *Nodal* in crown cells is induced by Notch signaling (Krebs et al., 2003; Przemeck et al., 2003). Unexpectedly, we found that *Wnt3* expression in the node is also directly induced by Notch signaling. We identified an enhancer in intron 2 of *Wnt3* that contains two Rbpj binding sites as the node crown cell enhancer (NDCE), and the expression of *Wnt3* was abolished by brief exposure of embryos to DAPT. Importantly, the expression of

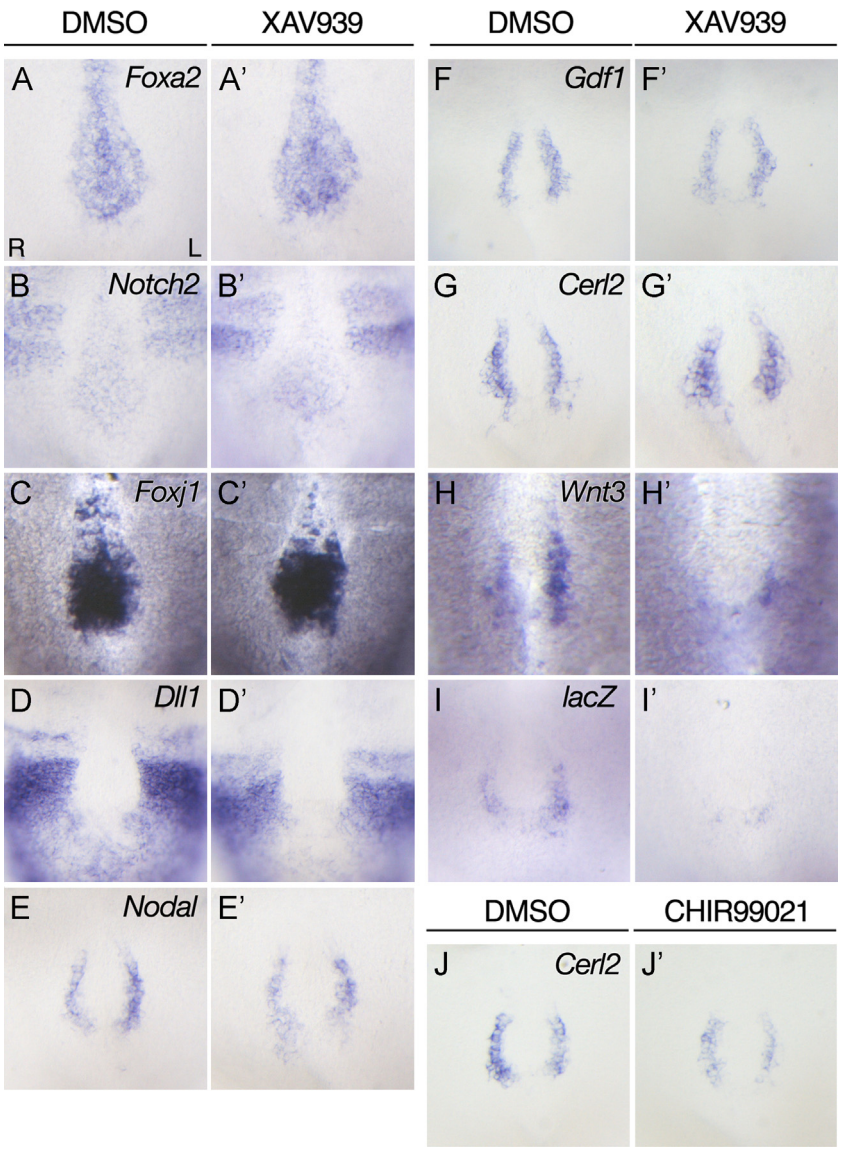


**Fig. 7.** The canonical Wnt signaling pathway regulates L–R asymmetry of *Cerl*2 expression. Expression of *Foxa*2 (A, A′), *Notch*2 (B, B′), *Foxj*1 (C, C′), *Dll*1 (D, D′), *Nodal* (E, E′), *Gdf*1 (F, F′), *Cerl*2 (G, G′, J, J′), *Wnt*3 (H, H′), and *lacZ* as a reporter for *Wnt*3 (I, I′) in wild-type (B, B′, H, H′) or $Wnt3^{NDCE\text{-}flox}$::*lacZ* transgenic (A, A′, C–G, C′–G′, I, I′, J, J′) embryos was examined by whole-mount in situ hybridization after culture from the one-somite stage to the three-somite stage in the presence of dimethyl sulfoxide vehicle (A–J), XAV939 (A′–I′), or CHIR99021 (J′). The node region is shown with anterior to the top.

*Gdf*1 and *Cerl*2 was also eliminated by DAPT treatment, suggesting that these genes may also be expressed in crown cells under the direct or indirect control of Notch signaling. Although DAPT is widely applied to inhibit Notch signaling, other effects of γ-secretase inhibition by this agent cannot be excluded. Further studies are thus required to confirm the regulation of *Gdf*1 and *Cerl*2 expression by Notch signaling in the node. Given that strict regulation of Nodal activity in the node is fundamental to L–R axis formation (Kawasumi et al., 2011; Marques et al., 2004; Tanaka et al., 2007), it is possible that this Notch-dependent mechanism may have developed to synchronize the expression of these genes in the same place.

Our study has also revealed that full activation of *Wnt*3 NDCE requires a Foxa2 binding site, which is sandwiched between the two Rbpj binding sites. Mutation of the Rbpj binding sites conferred ectopic enhancer activity in the pit cells of the node in a manner dependent on the Foxa2 binding site. A similar phenomenon was also observed for *Nodal* NDE, with mutation of the Rbpj binding sites also conferring *lacZ* expression in the pit cells. In the absence of Notch signaling, Rbpj recruits corepressors to silence gene expression in cultured cells (Borggrefe and Oswald, 2009). Given that the full activity of NDCE requires the Foxa2 binding site, its activation in pit cells is likely suppressed by Rbpj. In addition, the combination of Rbpj and Foxa2 is likely crucial for restriction of *Wnt*3 expression to crown cells, given that these cells are not the only ones in which Notch signaling occurs. We searched for enhancers of *Cerl*2 and *Gdf*1 by focusing on the combination of Foxa2 and Rbpj binding sites, but we were not able to identify such an enhancer. The partner of Rbpj in regulation of gene expression in crown cells may not necessarily be Foxa2, with other transcription factors expressed in the node also being candidates for such a partner.

Among secreted factors expressed in the node, the operation of two signaling pathways activated by such factors has been found to be L–R asymmetric in crown cells. First, phosphorylated Smad2 has been detected in crown cells on the left side (Kawasumi et al., 2011). This phosphorylation is dependent on the presence of Cryptic, indicating that Nodal in the node signals on the left side. Second, an increased level of β-catenin has been observed in the node, including crown cells, on the left side (Nakaya et al., 2005).

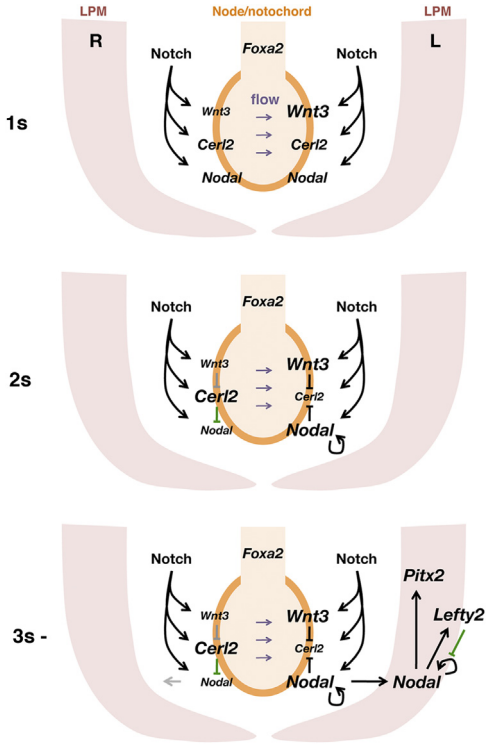


**Fig. 8.** Model for initial determination of the L–R axis around the node. The node region of the mouse embryo is shown schematically as viewed from the ventral side. The orange area represents the crown cells. The expression domains of *Wnt*3 and *Nodal* are determined by the combined action of Foxa2 and Rbpj under the control of Notch signaling. *Wnt*3 expression becomes stronger on the left side, which may result in greater suppression of *Cerl*2 expression on this side. At the two-somite (2s) stage, *Nodal* and *Cerl*2 establish opposite L–R asymmetric expression patterns, with Nodal activity thus becoming dominant on the left side. The LPM senses Nodal from the node first on the left side at the three-somite stage, with *Nodal* expression becoming amplified in the left LPM and resulting in the induction of *Pitx*2 expression. Green lines indicate suppression of protein activity, whereas black lines indicate the induction or suppression of gene expression. The reaction-diffusion of Nodal and Lefty across the embryo is omitted for simplicity. See Discussion for further details.

β-catenin is a central component of the canonical Wnt signaling pathway, and the expression pattern of Wnt3 suggests that this ligand may contribute to such asymmetry of canonical Wnt signaling. Do these signaling pathways contribute to the establishment of L–R asymmetric gene expression in the node? Importantly, the asymmetry of *Nodal* and *Cerl*2 expression in the node is not affected in *Cryptic*$^{-/-}$ embryos (Oki et al., 2009; Yan et al., 1999), indicating that Nodal signaling is dispensable for the asymmetric expression of both genes. As for canonical Wnt signaling, Wnt3a in the primitive streak maintains the expression of *Dll*1 and is therefore required for the expression of *Nodal* in crown cells (Nakaya et al., 2005). In the present study, our examination of the effects of potent compounds in whole-embryo culture without influencing *Nodal* expression showed that *Cerl*2 expression is augmented or attenuated as a result of inhibition or activation of canonical Wnt signaling, respectively. Although the expression domain of *Cerl*2 itself varies among embryos at the early somite stages (Supplementary Fig. S1), the asymmetry of *Cerl*2 expression is consistently established around the two-somite stage. Canonical Wnt signaling may confer the robust asymmetry of *Cerl*2 expression while overriding the native variation in the *Cerl*2 expression domain. Given that *Wnt*3 null mutant embryos exhibit early gastrulation defects (Liu et al., 1999), it remains to be determined whether Wnt3 regulates the asymmetry of *Cerl*2 expression. However, the expression pattern of *Wnt*3 suggests that the encoded protein may be a candidate regulator of asymmetric *Cerl*2 expression. Furthermore, we found that *Wnt*3 expression was greatly reduced as a result of inhibition of canonical Wnt signaling. Although we found that Notch signaling was inhibited slightly in embryos in which canonical Wnt signaling was blocked, the associated down-regulation of *Wnt*3 expression far exceeded that of other Notch-dependent genes such as *Nodal* and *Gdf*1, suggesting that the canonical Wnt pathway directly or indirectly increases *Wnt*3 expression.

On the basis of the results of the present study, we propose a model for regulation of asymmetric gene expression in crown cells of the node (Fig. 8). The expression of *Nodal*, *Cerl*2, *Gdf*1, and *Wnt*3 is induced by Notch signaling, and the specificity of the expression domains is ensured by the combination of Rbpj and other transcription factors functioning in the node. Nodal flow first generates asymmetric *Wnt*3 expression by an unknown mechanism. The expression of *Cerl*2 is suppressed by canonical Wnt signaling to a greater extent on the left side than on the right as a result of asymmetric *Wnt*3 expression. *Nodal* expression becomes up-regulated on the left side in a manner dependent on the *Nodal* intronic enhancer (Norris et al., 2002). The expression of *Nodal* and that of *Cerl*2 thus acquire opposite asymmetries in the crown cells, resulting in the generation of a difference in the distribution of active Nodal sufficient for the left LPM to respond first to Nodal signaling and thereby to allow L–R axis formation.

## Acknowledgments

We thank Y. Honda and Y. Nakajo for technical assistance; S. Nonaka for advice on observation of nodal flow; H. Sasaki, P. Chambon, T. Honjo, and S. Nagata for providing expression vectors; and S. Creekmore for providing recombineering reagents. The NICD expression plasmid was provided by the RIKEN BRC through the National Bio-Resource Project of the Ministry of Education, Culture, Sports, Science, and Technology of Japan. We also appreciate the technical support provided by the Research Support Center, Graduate School of Medical Sciences, Kyushu University. This work was supported by KAKENHI grants 21116002, 23570233, and 23770254 from the Japan Society for the Promotion of Science.

## Appendix A. Supporting information

Supplementary data associated with this article can be found in the online version at http://dx.doi.org/10.1016/j.ydbio.2013.05.011.

## References

Bain, J., Plater, L., Elliott, M., Shpiro, N., Hastie, C.J., McLauchlan, H., Klevernic, I., Arthur, J.S., Alessi, D.R., Cohen, P., 2007. The selectivity of protein kinase inhibitors: a further update. Biochem. J. 408, 297–315.
Bellomo, D., Lander, A., Harragan, I., Brown, N.A., 1996. Cell proliferation in mammalian gastrulation: the ventral node and notochord are relatively quiescent. Dev. Dyn. 205, 471–485.
Borggrefe, T., Oswald, F., 2009. The Notch signaling pathway: transcriptional regulation at Notch target genes. Cell Mol. Life Sci. 66, 1631–1646.
Brennan, J., Norris, D.P., Robertson, E.J., 2002. Nodal activity in the node governs left–right asymmetry. Genes Dev. 16, 2339–2344.
Caron, A., Xu, X., Lin, X., 2012. Wnt/beta-catenin signaling directly regulates Foxj1 expression and ciliogenesis in zebrafish Kupffer's vesicle. Development 139, 514–524.
Chen, F., Zhu, Y., Tang, X., Sun, Y., Jia, W., Han, X., 2011. Dynamic regulation of PDX-1 and FoxO1 expression by FoxA2 in dexamethasone-induced pancreatic beta-cells dysfunction. Endocrinology 152, 1779–1788.
Collignon, J., Varlet, I., Robertson, E.J., 1996. Relationship between asymmetric nodal expression and the direction of embryonic turning. Nature 381, 155–158.
Feller, J., Schneider, A., Schuster-Gossler, K., Gossler, A., 2008. Noncyclic Notch activity in the presomitic mesoderm demonstrates uncoupling of somite compartmentalization and boundary formation. Genes Dev. 22, 2166–2171.

Huang, S.M., Mishina, Y.M., Liu, S., Cheung, A., Stegmeier, F., Michaud, G.A., Charlat, O., Wiellette, E., Zhang, Y., Wiessner, S., Hild, M., Shi, X., Wilson, C.J., Mickanin, C., Myer, V., Fazal, A., Tomlinson, R., Serluca, F., Shao, W., Cheng, H., Shultz, M., Rau, C., Schirle, M., Schlegl, J., Ghidelli, S., Fawell, S., Lu, C., Curtis, D., Kirschner, M.W., Lengauer, C., Finan, P.M., Tallarico, J.A., Bouwmeester, T., Porter, J.A., Bauer, A., Cong, F., 2009. Tankyrase inhibition stabilizes axin and antagonizes Wnt signalling. Nature 461, 614–620.

Kato, H., Sakai, T., Tamura, K., Minoguchi, S., Shirayoshi, Y., Hamada, Y., Tsujimoto, Y., Honjo, T., 1996. Functional conservation of mouse Notch receptor family members. FEBS Lett. 395, 221–224.

Kawasumi, A., Nakamura, T., Iwai, N., Yashiro, K., Saijoh, Y., Belo, J.A., Shiratori, H., Hamada, H., 2011. Left–right asymmetry in the level of active Nodal protein produced in the node is translated into left–right asymmetry in the lateral plate of mouse embryos. Dev. Biol., 353; pp. 321–330.

Krebs, L.T., Iwai, N., Nonaka, S., Welsh, I.C., Lan, Y., Jiang, R., Saijoh, Y., O'Brien, T.P., Hamada, H., Gridley, T., 2003. Notch signaling regulates left–right asymmetry determination by inducing Nodal expression. Genes Dev. 17, 1207–1212.

Liu, P., Wakamiya, M., Shea, M.J., Albrecht, U., Behringer, R.R., Bradley, A., 1999. Requirement for Wnt3 in vertebrate axis formation. Nat. Genet. 22, 361–365.

Lowe, L.A., Supp, D.M., Sampath, K., Yokoyama, T., Wright, C.V., Potter, S.S., Overbeek, P., Kuehn, M.R., 1996. Conserved left–right asymmetry of nodal expression and alterations in murine situs inversus. Nature 381, 158–161.

Lubman, O.Y., Ilagan, M.X., Kopan, R., Barrick, D., 2007. Quantitative dissection of the Notch:CSL interaction: insights into the Notch-mediated transcriptional switch. J. Mol. Biol. 365, 577–589.

Marques, S., Borges, A.C., Silva, A.C., Freitas, S., Cordenonsi, M., Belo, J.A., 2004. The activity of the Nodal antagonist Cerl-2 in the mouse node is required for correct L/R body axis. Genes Dev. 18, 2342–2347.

McGrath, J., Somlo, S., Makova, S., Tian, X., Brueckner, M., 2003. Two populations of node monocilia initiate left–right asymmetry in the mouse. Cell 114, 61–73.

Meno, C., Shimono, A., Saijoh, Y., Yashiro, K., Mochida, K., Ohishi, S., et al., 1998. lefty-1 is required for left–right determination as a regulator of lefty-2 and nodal. Cell 94, 287–297.

Meno, C., Takeuchi, J., Sakuma, R., Koshiba-Takeuchi, K., Ohishi, S., Saijoh, Y., Miyazaki, J., ten Dijke, P., Ogura, T., Hamada, H., 2001. Diffusion of nodal signaling activity in the absence of the feedback inhibitor Lefty2. Dev. Cell 1, 127–138.

Mizushima, S., Nagata, S., 1990. pEF-BOS, a powerful mammalian expression vector. Nucleic Acids Res. 18, 5322.

Morohashi, Y., Kan, T., Tominari, Y., Fuwa, H., Okamura, Y., Watanabe, N., Sato, C., Natsugari, H., Fukuyama, T., Iwatsubo, T., Tomita, T., 2006. C-terminal fragment of presenilin is the molecular target of a dipeptidic γ-secretase-specific inhibitor DAPT (N-[N-(3,5-difluorophenacetyl)-L-alanyl]-S-phenylglycine t-butyl ester. J. Biol. Chem. 281, 14670–14676.

Nakamura, T., Mine, N., Nakaguchi, E., Mochizuki, A., Yamamoto, M., Yashiro, K., Meno, C., Hamada, H., 2006. Generation of robust left–right asymmetry in the mouse embryo requires a self-enhancement and lateral-inhibition system. Dev. Cell 11, 495–504.

Nakaya, M.A., Biris, K., Tsukiyama, T., Jaime, S., Rawls, J.A., Yamaguchi, T.P., 2005. Wnt3a links left–right determination with segmentation and anteroposterior axis elongation. Development 132, 5425–5436.

Nonaka, S., Tanaka, Y., Okada, Y., Takeda, S., Harada, A., Kanai, Y., Kido, M., Hirokawa, N., 1998. Randomization of left–right asymmetry due to loss of nodal cilia generating leftward flow of extraembryonic fluid in mice lacking KIF3B motor protein. Cell 95, 829–837.

Norris, D.P., Brennan, J., Bikoff, E.K., Robertson, E.J., 2002. The Foxh1-dependent autoregulatory enhancer controls the level of nodal signals in the mouse embryo. Development 129, 3455–3468.

Oki, S., Hashimoto, R., Okui, Y., Shen, M.M., Mekada, E., Otani, H., Saijoh, Y., Hamada, H., 2007. Sulfated glycosaminoglycans are necessary for nodal signal transmission from the node to the left lateral plate in the mouse embryo. Development 134, 3893–3904.

Oki, S., Kitajima, K., Marques, S., Belo, J.A., Yokoyama, T., Hamada, H., Meno, C., 2009. Reversal of left–right asymmetry induced by aberrant nodal signaling in the node of mouse embryos. Development 136, 3917–3925.

Overdier, D.G., Porcella, A., Costa, R.H., 1994. The DNA-binding specificity of the hepatocyte nuclear factor 3/forkhead domain is influenced by amino-acid residues adjacent to the recognition helix. Mol. Cell. Biol. 14, 2755–2766.

Pearce, J.J., Penny, G., Rossant, J., 1999. A mouse cerberus/Dan-related gene family. Dev. Biol. 209, 98–110.

Przemeck, G.K., Heinzmann, U., Beckers, J., Hrabe de Angelis, M., 2003. Node and midline defects are associated with left–right development in Delta1 mutant embryos. Development 130, 3–13.

Rankin, C.T., Bunton, T., Lawler, A.M., Lee, S.J., 2000. Regulation of left–right patterning in mice by growth/differentiation factor-1. Nat. Genet. 24, 262–265.

Raya, A., Kawakami, Y., Rodriguez-Esteban, C., Buscher, D., Koth, C.M., Itoh, T., Morita, M., Raya, R.M., Dubova, I., Bessa, J.G., de la Pompa, J.L., Izpisua Belmonte, J.C., 2003. Notch activity induces nodal expression and mediates the establishment of left–right asymmetry in vertebrate embryos. Genes Dev. 17, 1213–1218.

Saijoh, Y., Adachi, H., Sakuma, R., Yeo, C.Y., Yashiro, K., Watanabe, M., Hashiguchi, H., Mochida, K., Ohishi, S., Kawabata, M., Miyazono, K., Whitman, M., Hamada, H., 2000. Left–right asymmetric expression of lefty2 and nodal is induced by a signaling pathway that includes the transcription factor FAST2. Mol. Cell 5, 35–47.

Saijoh, Y., Oki, S., Ohishi, S., Hamada, H., 2003. Left–right patterning of the mouse lateral plate requires nodal produced in the node. Dev. Biol. 256, 160–172.

Sasaki, H., Hogan, B.L., 1993. Differential expression of multiple fork head related genes during gastrulation and axial pattern formation in the mouse embryo. Development 118, 47–59.

Scott, G.K., Daniel, J.C., Xiong, X., Maki, R.A., Kabat, D., Benz, C.C., 1994. Binding of an ETS-related protein within the DNase I hypersensitive site of the HER2/neu promoter in human breast cancer cells. J. Biol. Chem. 269, 19848–19858.

Shiratori, H., Hamada, H., 2006. The left–right axis in the mouse: from origin to morphology. Development 133, 2095–2104.

Sulik, K., Dehart, D.B., Iangaki, T., Carson, J.L., Vrablic, T., Gesteland, K., Schoenwolf, G.C., 1994. Morphogenesis of the murine node and notochordal plate. Dev. Dyn. 201, 260–278.

Tanaka, C., Sakuma, R., Nakamura, T., Hamada, H., Saijoh, Y., 2007. Long-range action of Nodal requires interaction with GDF1. Genes Dev. 21, 3272–3282.

Tanaka, Y., Okada, Y., Hirokawa, N., 2005. FGF-induced vesicular release of Sonic hedgehog and retinoic acid in leftward nodal flow is critical for left–right determination. Nature 435, 172–177.

Tun, T., Hamaguchi, Y., Matsunami, N., Furukawa, T., Honjo, T., Kawaichi, M., 1994. Recognition sequence of a highly conserved DNA binding protein RBP-J kappa. Nucleic Acids Res. 22, 965–971.

Walentek, P., Beyer, T., Thumberger, T., Schweickert, A., Blum, M., 2012. ATP4a is required for Wnt-dependent Foxj1 expression and leftward flow in Xenopus left–right development. Cell Rep. 1, 516–527.

Yamamoto, M., Mine, N., Mochida, K., Sakai, Y., Saijoh, Y., Meno, C., Hamada, H., 2003. Nodal signaling induces the midline barrier by activating nodal expression in the lateral plate. Development 130, 1795–1804.

Yan, Y.T., Gritsman, K., Ding, J., Burdine, R.D., Corrales, J.D., Price, S.M., Talbot, W.S., Schier, A.F., Shen, M.M., 1999. Conserved requirement for EGF-CFC genes in vertebrate left–right axis formation. Genes Dev. 13, 2527–2537.